

# Design and Development of a Sub-1 kg Wall-Climbing Robot Using Electric Ducted Fan for Vertical Surface Operations

Maddi Srihitha  
B.E Student

Department of Mechanical Engineering,  
Chaitanya Bharathi Institute of  
Technology  
Hyderabad, India

Mallela Sriharinath  
B.E Student

Department of Mechanical Engineering,  
Chaitanya Bharathi Institute of  
Technology  
Hyderabad, India

Mogulla Dhruva  
B.E Student

Department of Mechanical Engineering,  
Chaitanya Bharathi Institute of  
Technology  
Hyderabad, India

Ch. Indira Priyadarshini  
Assistant professor

Department of Mechanical Engineering,  
Chaitanya Bharathi Institute of  
Technology  
Hyderabad, India

**Abstract** - This paper will show the design and development of a miniature wall-climbing robot with the help of Electric Ducted Fan (EDF) suction adhesion into the role of robot in the vertical plane. It has a light-weight system that includes surface cleaning and optical inspection. These include: (1) a multipurpose platform was designed with a minimum footprint; (2) cleaning and inspection was added to a sub-1 kg platform; (3) hybrid sealing mechanism was created to have optimal air gap; (4) simplified control architecture was made in order to provide fail-safe adhesion; and (5) analytical models were developed. Theoretical analysis confirms that the total adhesion force is approximately 14 N at the operating throttle, validated by CFD simulation of the EDF-skirt assembly. The hybrid sealing system provides integrity of negative pressure chambers and the control system separates the role of adhesion-critical functions and fail to compute. The design and theoretical analysis is presented in this paper.

**Keywords** - *Electric Ducted Fan (EDF), fail-safe control system, hybrid rigid connection, suction adhesion.*

## I. INTRODUCTION

Robots mounted on walls have joined the enabling robots during the inspections and cleaning up of tall walls whose use is deemed hazardous and whose operation is deemed complex in case of human access. Conventional techniques are tedious, take up a lot of time and put workers at risk of falls. WCRS minimize these limitations to uses like building

facade maintenance, bridge inspection and infrastructure monitoring.

There are various mechanisms of wall-climbing robot adhesion, such as magnetic adhesion, vacuum suction, dry adhesives, and propeller thrust. Non-ferromagnetic smooth surfaces like glass and painted walls can be utilized with Electric Ducted Fan (EDF) type and have the benefit of having a continuous adhesion without surface preparation.

Various degrees of integration exist in EDF robots in the present scenario. Past efforts had resulted in both thermal-inspection robots that failed at cleaning and other platforms with good climbing capabilities at demonstrated force analysis, but without vision.

The project develops a small and highly versatile wall-climber robot characterized by a combination of EDF-based adhesion, a locomotion based on wheels and an overall mass of less than 1 kg. The project has had the following significant contributions: (1) dimensional optimization of the system: to realize a high level of footprint and mass reduction; (2) integration of EDF-based adhesive with wheel-driven locomotion; (3) integration of pressure-force relationships with consideration of leakage to enable the application to practical deployment conditions.

## II. LITERATURE REVIEW

### A. Taxonomical Classification of Wall-Climbing Robots

Nansai and Mohan [1] reported a taxonomical survey of robots based on their adhesion mechanisms, wall-climbing robots into six different classes mentioned as suction cup adhesion, suction cup crawler, vacuum pump adhesion, magnetic adhesion, propeller-thrust adhesion, and bio-

inspired adhesion. According to their review, a gap in the literature was found: all the existing platforms are usually ready to perform one mode of functioning, and the integrated cleaning-and-climbing systems are not widely represented.

### B. Design Optimization of Indoor Wall-Climbing Robots

Zheng et al. [5] invented an indoor wall-climbing This type of robotic inspection system which uses a QF2611 EDF single unit (70 mm diameter, 4600 kV) and features an integrated thermal imaging system. Their platform weighed a total of 538 g and was 228 x 190 x 110 mm. Above all, they discovered in the experiment of deploying a small wheel diameter (under 45 mm) reduces the chassis-to-wall clearance that promotes the volumetric efficiency of the suction chute. Micro geared DC motor with wheels (43 mm in diameter) proved to be the best motor to adopt in compact geometries: GA12-N20.

### C. Force and Torque Analysis for Vertical Climbing

Vangala et al. [3] offered strict force balance analysis, resulting in the basic torque estimation deriving the fundamental torque requirement:  $T_m \geq (\mu F_s + W) \times r_w$ , where  $\mu$  denotes static friction coefficient,  $F_s$  represents suction force,  $W$  is robot weight, and  $r_w$  is wheel radius. Their 1500 g platform validated successful vertical climbing using six drive motors.

### D. Adhesion and Suction Performance

Andrikopoulos et al. [4] experimented with the vortex adhesion dynamic of the 92 mm EDF, shroud geometry of their own design. The stationary condition, which they employed, was to ascertain the coefficient of friction of 0.82 between two rubber wheels and painted surfaces, which is quite high as compared to the ordinary coefficient of friction which is supposed to be 0.6. Urban et al. [6] came up with the idea that a square geometry of the shroud has approximately 16 percent higher suction forces relative to a circular geometry and that optimum operation in the operation of the vortex mechanisms can be achieved where there is a wall gap spaced at about 89 mm.

## III. METHODOLOGY

### A. Design Philosophy and Optimization Constraints

The design strategy aimed at three primary objectives: (1) low footprint, with no loss in functional completeness; (2) low total mass (below 1 kg) and this provides higher adhesion safety margin; and (3) the modular architecture enabling the future scaling of capabilities. Weight estimation of the bot is lower than the weight of 1 kg; depending on the characteristics of EDF thrusts in literature, and the desired safety factor of 1.5x. Components were selected based on systematic mass-versatility. The design use was on the concept of concurrent engineering whereby it went through

the process of CAD modelling in SolidWorks, iterative design validation and fabrication of the prototype.

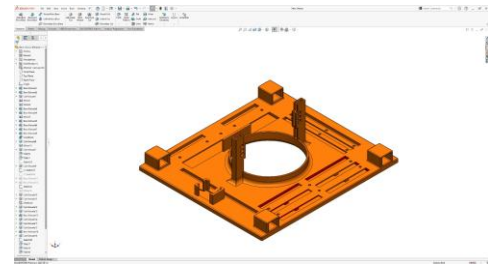


Fig 1: Chassis Design in Solidworks

### B. Mechanical Structure Design

The Polylactic Acid fabricated body via Fused Deposition Modelling (FDM) has approximate dimensions 200x 180mm Chassis platform and parametric slot patterns removed material, which reduces the chassis mass, without reducing its structural integrity. A negative pressure chamber is constructed into the underbody and is a square. The concern of component layout is to concentrate the mass of such components about geometric centreline to reduce peeling caused by vertical operation. The total chassis height is lower than compared to the platform as reported by Zheng et al. [5].

### C. Negative Pressure Adhesion System

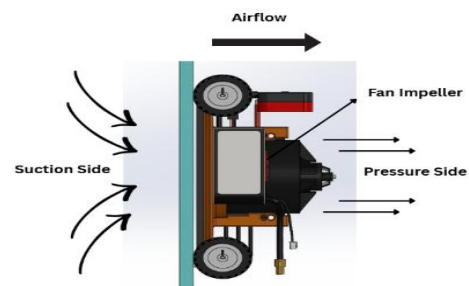


Fig 2: EDF Based Adhesion system

This principle of adhesion utilises a Powerfun 70 mm CCW EDF engine with 2300 kV brushless motor powered by 4S LiPo battery. The operation of the motor is regulated by an 80A brushless ESC. The hybrid sealing is one of the methods, which address air leakage. It consists of 3D printed TPU material to make the main seal. The step of secondary sealing suggests applying 2 mm silicone foam tape to the airtight perimeter of the skirt which focuses on irregularities in the surface as well as assures of the integrity of seals. The double layer design permits the integrity of the seal even when there is a surface variation, as well as lessening friction. A 3 mm skirt-to-wall sealing distance reduces peripheral leakage with the appropriate amount of chamber height at 15.45 mm chassis-to-wall chamber height which involves a skirt of 12.45 mm and then 3 mm from skirt to wall giving internal volume needed to create and develop low-pressure vortices.

### D. Locomotion and Drive System

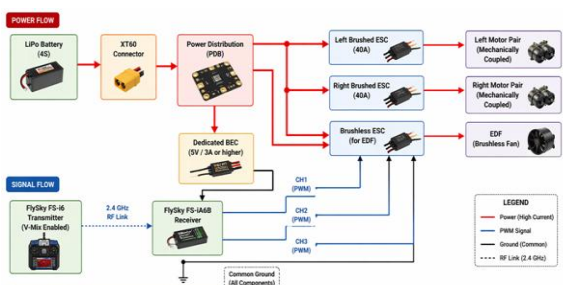


Fig 3: Control Architecture Block Diagram

The process of steering is attained through 4 micro geared DC motors ( 6 V, 30 RPM, 10 kg-cm stall torque) in a differential drive, with left/right pairs, which are mechanically coupled, instead of complex kinematics of traditional steering. These wheels (55 mm large of the wheel/20 mm wide) are planned with the principle of optimization proposed by Zheng et al. [5]: the lesser is the diameter of the wheel, the little is the clearance of the chassis and the walls, the bigger is the chamber performance.

### E. Fail-Safe Control Architecture

Such design is a unique one when compared to all the known WCRs that are based on microcontrollers [3][5][6] since it has the zero-MCU motor control architecture. Transmitter-side V-tail mixing on FlySky FS-i6 provides differentials on steering which were played out to the ESCs without computation. This guarantees the adhesion-critical EDF and locomotion is not reliant on an onboard computer. Raspberry Pi Zero 2W can be used as an isolated intelligence tier, and it does not have control over actuators of safety-critical features to guarantee that they obey the commands during compute errors.

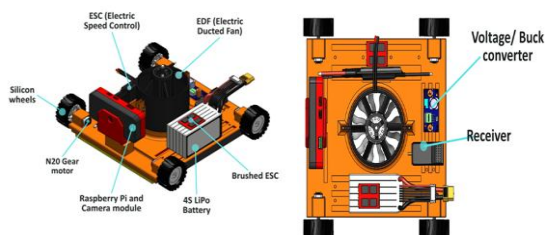


Fig 4: System Architecture: Components & Electrical Layout

### F. Vision and Inspection Subsystem

The 8-megapixel (3280x 2464, 79.3 o FOV) sensor is Sony IMX219 and is attached to Raspberry Pi Zero 2W by CSI. Its features of functionality include H.264 video streaming over Wi-Fi, high-resolution still-capture, and an on-board TensorFlow Lite inference to identify defects. They can be avoided by isolation of power by exclusive LM2596 buck converter (5.1V) to prevent the effect of transient EDF voltage changes on the stability of the compute. The camera has likewise been mounted on rotational servo mount which

can swivel up to 180 degrees in the horizontal direction. With thermo-imaging (80x60 px), Zheng et al. provide a much less developed image compared to this 8 MP photo. [5]

### G. Cleaning Mechanism

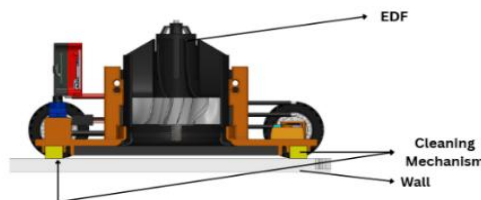


Fig 5: Employed Cleaning Mechanism

It has a cleaning mechanism with 2 underside mounted cleaning blocks (modular cleaning pad) which is melamine foam layer overlaid on EVA backing and can be easily replaced and provides effective and consistent cleaning of the surface. They are placed in a symmetric manner on either sides of the centreline, they can be cleaned equally and the stability of the system maintained in case there is vertical movement. The blocks are passive, implying that they do not require additional actuators in eliminating dust and debris, therefore, reducing the power used.

### H. Wheel Specifications

A 55 mm silicone tire (Shore A 35) with a hexagonal hub was custom-cast using a 3D-printed mould to achieve the required tread profile and durometer. The cast wheel is connected to the N20 motor shaft through a 3D-printed adapter, replacing the press-fit coupling that degraded in previous iterations. The silicone tread provides reliable grip across painted wall, concrete, and tile surfaces ( $\mu = 0.73-0.88$ ), while the hexagonal geometry ensures consistent torque transfer without slippage.

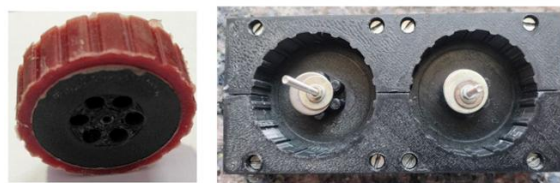


Fig 6: 55mm Wheels with Silicone Tread (Left) Silicone Wheel mould Cavity (Right)

## IV. SYSTEM SPECIFICATIONS

Table I summarizes technical specifications in detail such as mechanical, electrical, computational and performance characteristics of the developed wall-climbing robot.

TABLE I: COMPLETE TECHNICAL SPECIFICATIONS

Technical Specifications	
Parameter	Specification
EDF Unit	Powerfun 70 mm CCW, 2300 kV BLDC, 12 blades Fan
Battery Pack	4S 1550 mAh 100C LiPo (14.8V nominal)
Drive Motors	4× GA12-N20, 6V, 30 RPM, 10 kg-cm
Servo Motor	SG90 servo motor, 4.8V, 180 degrees
Wheel Specifications	55 mm Ø × 20 mm, silicone rubber tread
Sealing System	TPU (Shore A 85) + 2 mm (silicone foam compliant seal)
Chamber height	15.45 mm (skirt thickness of 12.45 mm, a 3 mm gap between wall and skirt surface.)
Vision Module	Sony IMX219, 8 MP, 79.3° FOV
Compute Module	Raspberry Pi Zero 2W (1 GHz, 512 MB)
RC System	FlySky FS-i6 TX + FS-iA6B RX (2.4 GHz)

## V. THEORETICAL ANALYSIS

### A. Pressure-Force Relations

The basic correlation governing the EDF adhesion is based on the equation of Pressure- Force:

$$F_{\text{adhesion}} = \Delta P \cdot A \quad (1)$$

$F_{\text{adhesion}}$  is the force of adhesion in Newtons, [ $dP$  -pa atm] the difference of pressure between the inside and the atmosphere pressure in Pascals, and [ $A$ -effective suction area in square meters]. This is the model which is typical in negative-pressure adhesion systems and it has been experimentally verified by Andrikopoulos et al. [4] and by Zheng et al. [5].

In the case of a vertical robot, no-slip condition means that the friction force must match or exceed weight:

$$F_f \geq W \quad (2)$$

and  $F_f = \mu N$  = friction force,  $N$  = normal force (equal to adhesion force  $F_s$ ) and  $W = mg$ , weight of robot. When these relationships are combined, they result in the least needed force in adhesion:

$$F_{s,\text{min}} = W/\mu = mg/\mu \quad (3)$$

The use of safety factor  $n$  to consider the uncertainties and dynamic effects practiced during climbing:

$$F_{s,\text{design}} = n \cdot F_{s,\text{min}} \quad (4)$$

### B. Wheel Torque Validation

The wheel torque value is based on the traction force required to easily climb vertically. Following Vangala et al. [3]:

$$\tau = F_t \cdot r_w = (\mu N) \cdot r_w \quad (5)$$

The stall torque of each N20 micro gear motor is 10 kg-cm or about 0.314 N-m per motor. By using 4 motors to move the platform, the amount of available torque is 1.26 N.m, a factor 8.12x more than the required wheel torque. This margin allows a sure vertical climbing without slipping of the wheels even during the transient loading conditions.

The basic analytical correlations and the final results obtained through the application of the corresponding formulas of the generated adhesion forces of a platform in question, mechanics of friction as well as the need to introduce the drive-torques into the theoretical analysis of the wall-climbing robot are supported in Table II.

TABLE II: THEORETICAL FORMULAS

Theoretical Formulae	
Parameter	Formula
Robot Weight	$W = mg = 8.34 \text{ N}$
Friction Force	$F_f = \mu N; \mu = 0.6$
Friction Force Condition	$F_f \geq W$ (Satisfied)
Minimum Suction Force	$F_{s,\text{min}} = mg/\mu = 13.9 \text{ N}$
Design Adhesion Force	$F_{s,\text{design}} = n \cdot F_{s,\text{min}} = 20.85 \text{ N}$ ( $n = 1.5$ )
Wheel Torque (per wheel)	$\tau = F_t \cdot r_w = 0.1216 \text{ N}\cdot\text{m}$
Traction force per wheel	$F_t = \mu \cdot N / 4 = 4.17 \text{ N}$

## VI. RESULTS

### [1] Assembled Prototype and System Integration

The final assembled prototype mounted on a vertical wall surface is shown in Fig.9, demonstrating successful adhesion with all integrated subsystems visible including the EDF unit, drive wheels, sealing skirt, cleaning blocks, and camera module. The complete system weighs approximately 850 g, satisfying the sub-1 kg design target.

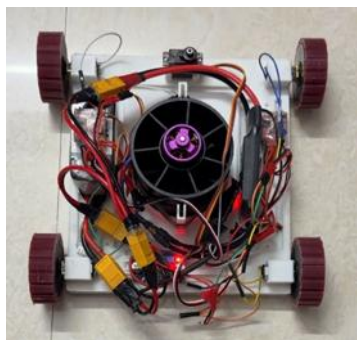


Fig 7: Assembled Prototype and System Integration

[2] CFD Validation of EDF-Skirt Assembly Performance

The EDF-skirt assembly was evaluated through steady-state CFD analysis in ANSYS Fluent. The 70 mm Powerfun EDF was modelled with a 12-blade rotor (1 mm thickness, 23° twist) coupled to the square underbody skirt, with a 3 mm skirt-to-wall sealing gap and a 12.45 mm chassis-to-wall chamber height. Boundary conditions replicated vertical-surface deployment. simulation yielded a suction force of 24 N, exceeding the 20.85 N design requirement design requirement defined in Section V. A real-world deviation of approximately ±5% is anticipated due to minor leakage at the skirt interface.



Fig 7a: EDF Fan



Fig 7b: Results of CFD Analysis of EDF

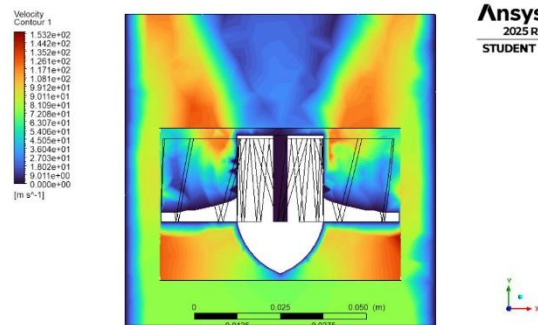


Fig 7c: Results of CFD Analysis of EDF

[3] Adhesion Performance in Relation to Design Goals

The total force of adhesion of 13.55 N (70% throttle) is higher than the minimum required force of 9.48 N ( $F_s, \min = W/\mu = 8.34/0.88$ ) with a safety factor of 1.43 confirming the design for textured indoor surfaces. The robot was able to climb reliably on concrete and painted walls. However, on smooth surfaces such as glass, the TPU skirt cannot provide sufficient sealing because the surface does not have micro-roughness and the chamber cannot maintain the adhesion threshold. Extending operation to glass surfaces, an open research gap, still requires compliance or surface-adaptive sealing. Testing on highly smooth surfaces such as glass and polished tile revealed that the robot was unable to sustain climbing due to insufficient wheel traction. The silicone tires (Shore A 35,  $\mu = 0.73$  on tile) could not generate adequate friction to satisfy the no-slip condition ( $F_f \geq W = 8.34$  N), with the effective friction force dropping to approximately 5.8 N on polished surfaces ( $\mu \approx 0.45$ ), falling below the 8.34 N threshold despite the EDF maintaining sufficient suction. This indicates the limitation is traction-based rather than adhesion-based, requiring surface-adaptive tread compounds to extend operation to smooth surfaces.

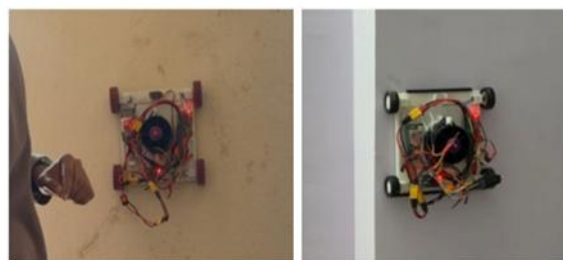


Fig 9: Working prototype on vertical wall

[4] Power System Adequacy and Operational Endurance

Battery characterisation confirmed approximately 5-6 minutes at 60% traversal throttle and 2-3 minutes at 80% maximum thrust. Peak transient current during EDF spool-up reached 110-130 A, representing approximately 70-85% of the battery's 155 A rated capacity. Compared to Zhang et al. (2025), who achieved approximately 10 minutes on a 538 g platform, the present system trades runtime for higher adhesion margin while carrying additional camera, compute, and cleaning payloads within a sub-1 kg budget.

### [5] Integration and Operational Observations

Camera integration performed reliably across all climbing trials, with consistent 30 FPS recording maintained throughout. No vibrational artifacts or image degradation were observed attributable to EDF or motor vibration, confirming the adequacy of the mechanical coupling strategy for shock isolation. The lightweight mounting bracket (<5 g) successfully minimised impact on adhesion margin and locomotion efficiency.

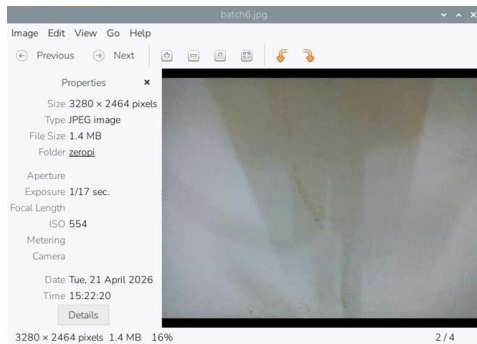


Fig 9: On-board camera image captured during climbing trial on painted wall.

Qualitative observations during climbing operations noted that differential drive steering kinematics functioned as designed, with independent left/right motor pair control enabling smooth trajectory correction without adhesion loss. No instances of uncontrolled descent or adhesion margin violation were recorded across any trial.

### B. Discussion

The experimental results suggest that the EDF-based negative pressure adhesion system provides a safe adhesion margin on a lightweight (less than 1 kg) robot platform, consistent with previous research that indicates an increase in adhesion efficiency for low mass-to-suction ratio systems in micro-scale wall-climbing robots. The measured power ( $\approx 120$ -130 W at  $\sim 60\%$  throttle) and endurance (6-8 minutes) are in line with the experimental results in EDF-based adhesion studies, where the energy efficiency is still a challenge due to the continuous airflow demand. The observed problems, such as wheel slipping on low coefficient of friction surfaces, seal wear, and heat increase in the EDF unit, are also shown in other negative pressure and vortex adhesion systems, highlighting a balance between adhesion performance and mechanical robustness. Additionally, the edge transition inability is a common issue in single module-based systems, as reported in previous studies, with multi-segment or hybrid adhesion strategies recommended for enhanced locomotion. These results not only confirm the design's feasibility but also highlight the importance of improvement in traction, sealing, and thermal issues to enable practical use.

### VII. CONCLUSION AND FUTURE WORK

The paper effectively presents the design and implementation of a lightweight, versatile wall-climbing robot with an Electric Ducted Fan (EDF)-based negative

pressure adhesion system, marking a significant advancement in the field of lightweight and energy efficient vertical robotics. The design offers a highly compact form factor, one of the smallest reported for EDF-based wall-climbing robots, and successfully integrates cleaning and high-resolution (8 MP) visual inspection functions into a lightweight (less than 1 kg) untethered system. The hybrid seal design, featuring a flexible TPU skirt and high-density silicone foam, improves adhesion performance under different surface textures, as reported in recent research on suction-based adhesion. Moreover, the use of a zero-MCU control with fail-safe adhesion capabilities simplifies the system design, minimises computational complexity, and enhances system robustness in critical adhesion scenarios.

In summary, this design offers a good balance between adhesion, mobility and functionality, and holds the potential for both commercial and domestic applications in façade cleaning, inspection and monitoring. The findings confirm the potential of EDF-based adhesion for lightweight robotic systems, and also contribute to current research directions in wall-climbing robots, with a focus on lightweight design and efficiency, energy efficiency, and multifunctionality.

Future research opportunities also add to the research contribution. Future experiments on different substrates such as glass, concrete, and rough surfaces will offer more insights into the system's performance and its adaptability for adhesion. The integration of autonomous locomotion with SLAM algorithms and defect detection with TensorFlow Lite classifiers will add to the system's autonomy and smartness. Moreover, improvements to the power system with a 6S battery configuration and thermal modelling during prolonged use will ensure longevity and stability. These enhancements will make the proposed system a flexible and expandable platform, with the potential to evolve into a field-ready wall-climbing robotic system

### VIII. ACKNOWLEDGEMENT

The authors wish to acknowledge the HoD and the project coordinators of The Department of Mechanical Engineering, Chaitanya Bharathi Institute of technology, Hyderabad, who provided invaluable guidance, tireless support, and healthy suggestions, during the duration of this project. The authors also recognize that they were supported by the Digital Fabrication Lab headed by Mr. K. Rajgopal of the Dept. of Mechanical Engineering of CBIT to support the resources and infrastructure needed.

### REFERENCES

- [1] S. Nansai and R. E. Mohan, "A survey of wall-climbing robots: Recent advances and challenges," *Robotics*, vol. 5, no. 3, pp. 1-33, July 2016.
- [2] L. Ma and T. Hartmann, "Exploration of using a wall-climbing robot system for indoor inspection in occupied buildings," *Scientific Reports*, vol. 14, article 13770, June 2024.
- [3] N. Vangala, C. Varunav, J. Aravind, S. M. Yasin, and E. M. Raju, "Design and analysis of wall-climbing robot," in *Proc. Second Int. Conf. Emerging Trends Engineering (ICETE 2023)*, November 2023.
- [4] G. Andrikopoulos and G. Nikolopoulos, "Vortex actuation via Electric Ducted Fans: An experimental study," *Journal of Intelligent & Robotic Systems*, vol. 95, pp. 955-973, September 2018.
- [5] Z. Zheng, S. Yang, P. Zhang, C. Xu, B. Li, and Y. Li, "Theoretical and simulation study of suction force in wall-climbing cleaning robots with

negative pressure adsorption," *Applied Sciences*, vol. 14, December 2024.

- [6] D. Urban, S. Kusmirek, V. Socha, L. Hanakova, K. Hylmar, and J. Kraus, "Effect of Electric Ducted Fans structural arrangement on their performance characteristics," *Applied Sciences*, vol. 13, February 2023.
- [7] Y. Fang, S. Wang, D. Cui, Q. Bi, R. Jiang, and C. Yan, "Design and optimization of wall-climbing robot impeller by genetic algorithm based on computational fluid dynamics and kriging model," *Scientific Reports*, vol. 12, article 9571, June 2022.
- [8] Y. Jin, Y. Qian, Y. Zhang, and W. Zhuge, "Modelling of ducted-fan and motor in an electric aircraft and a preliminary integrated design," *SAE Int. J. Aerospace*, vol. 11, no. 2, October 2018.
- [9] J. Guo and Z. Zhou, "An efficient blade design method of a ducted fan coupled with the CFD modification," *Aerospace*, vol. 9, April 2022.
- [10] R. Weinstein and B. M. Simmons, "Experimental characterization of an Electric Ducted Fans" NASA Langley Research Centre, Technical Report, January 2024.